Immunity
Article

A Clonogenic Progenitor with Prominent Plasmacytoid Dendritic Cell Developmental Potential

Nobuyuki Onai,[1,2] Kazutaka Kurabayashi,[1] Mayuka Hosoi-Amaike,[1] Noriko Toyama-Sorimachi,[3] Kouji Matsushima,[2,4] Kayo Inaba,[2,5] and Toshiaki Ohteki[1,2,*]
[1]Department of Biodefense Research, Medical Research Institute, Tokyo Medical and Dental University, Tokyo 113-8510, Japan
[2]Japan Science and Technology Agency, Core Research for Evolutional Science and Technology (CREST), Tokyo 102-0081, Japan
[3]Department of Molecular Immunology and Inflammation, Research Institute, National Center of Global Health and Medicine, Tokyo 162-8655, Japan
[4]Department of Molecular Preventive Medicine, Graduate School of Medicine, The University of Tokyo, Tokyo 113-0033, Japan
[5]Laboratory of Immunobiology, Department of Animal Development and Physiology, Division of Systemic Life Science, Graduate School of Biostudies, Kyoto University, Kyoto 606-8501, Japan
*Correspondence: ohteki.bre@mri.tmd.ac.jp
http://dx.doi.org/10.1016/j.immuni.2013.04.006

SUMMARY

Macrophage and dendritic cell (DC) progenitors (MDPs) and common DC progenitors (CDPs) are bone marrow (BM) progenitors with DC differentiation potential. However, both MDPs and CDPs give rise to large numbers of conventional DCs (cDCs) and few plasmacytoid DCs (pDCs), implying that more dedicated pDC progenitors remain to be identified. Here we have described DC progenitors with a prominent pDC differentiation potential. Although both MDPs and CDPs express the macrophage colony stimulating factor (M-CSF) receptor (M-CSFR), the progenitors were confined to a M-CSFR$^-$ fraction, identified as Lin$^-$c-Kit$^{int/lo}$Flt3$^+$M-CSFR$^-$, and expressed high amounts of *E2-2* (also known as *Tcf4*) an essential transcription factor for pDC development. Importantly, they appeared to be directly derived from either CDPs or lymphoid-primed multipotent progenitors (LMPPs). Collectively, our findings provide insight into DC differentiation pathways and may lead to progenitor-based therapeutic applications for infection and autoimmune disease.

INTRODUCTION

Dendritic cells (DCs) have crucial functions in the initiation of innate and adaptive immunity in infection and inflammation and in the induction of tolerance under steady-state conditions (Banchereau and Steinman, 1998). DCs consist of conventional DCs (cDCs) and plasmacytoid DCs (pDCs) (Banchereau and Steinman, 1998; Liu, 2005; Shortman and Naik, 2007; Geissmann et al., 2010; Swiecki and Colonna, 2010). pDCs are present in human (Siegal et al., 1999; Cella et al., 1999) and mouse (Asselin-Paturel et al., 2001; Nakano et al., 2001; Björck, 2001) and are characterized by their capacity to produce large amounts of type I interferons (IFNs) (Siegal et al., 1999; Cella et al., 1999; Asselin-Paturel et al., 2001; Nakano et al., 2001; Björck, 2001). The pDCs' activation and type I IFN production are critical for the initiation of antiviral immune responses, whereas pDCs' activation in the absence of infection causes autoimmune diseases, such as systemic lupus erythematosis (SLE) and psoriasis vulgaris (Gilliet et al., 2008; Banchereau and Pascual, 2006). In addition, local microenvironments can induce tolerogenic properties in pDCs (de Heer et al., 2004; Goubier et al., 2008). It was recently shown that basic helix-loop-helix transcription factor E2-2 (also known as TCF4) is essential for pDC development in both human and mouse (Nagasawa et al., 2008; Cisse et al., 2008) and maintenance of mature pDCs (Ghosh, et al., 2010).

DCs are originated from hematopoietic stem cells (HSCs) in the bone marrow (BM) via intermediate progenitors (Shortman and Naik, 2007; Geissmann et al., 2010; Merad and Manz, 2009). The intermediate sequential progenitors are classified on the basis of their chemokine and cytokine receptor expression and in vivo DC differentiation ability (Fogg et al., 2006; Auffray et al., 2009; Liu et al., 2009; Onai et al., 2007; Naik et al., 2007). Fms-like tyrosine kinase receptor-3 (Flt3) has a nonredundant role in the steady-state differentiation and maintenance of pDCs and cDCs in vivo. Mice deficient for Flt3 or Flt3-ligand (Flt3L) are poor producers of cDCs and pDCs in vivo (McKenna et al., 2000; Waskow et al., 2008), and the recently identified macrophage and DC progenitors (MDPs) and common DC progenitors (CDPs) express Flt3 on their cell surface (Cisse et al., 2008; Fogg et al., 2006; Auffray et al., 2009; Liu et al., 2009). MDPs express the phenotypic markers Lin$^-$CX$_3$CR1$^+$CD11b$^-$c-Kit$^+$Flt3$^+$M-CSFR$^+$ and produce macrophages and cDCs and pDCs through CDPs (Fogg et al., 2006; Onai et al., 2007; Naik et al., 2007; Auffray et al., 2009; Liu et al., 2009), whereas CDPs are Lin$^-$c-Kit$^{int/lo}$Flt3$^+$M-CSFR$^+$ cells that give rise exclusively to cDCs and pDCs (Onai et al., 2007; Naik et al., 2007), suggesting that CDPs are stringently committed to the DC lineage. The immediate cDC precursors, namely pre-DCs, which are derived from CDPs, migrate into lymphoid and some nonlymphoid tissues where they differentiate into cDCs (Naik et al., 2006, 2007; Varol et al., 2009; Bogunovic et al., 2009; Ginhoux et al., 2009). Notably, both MDPs and CDPs give rise to many fewer pDCs than cDCs. In this study, we identified DC-committed progenitors, i.e., Lin$^-$c-Kit$^{int/lo}$Flt3$^+$M-CSFR$^-$IL-7Rα^- cells, with prominent pDC differentiation potential, and our findings revise the current understanding of DC differentiation pathways.

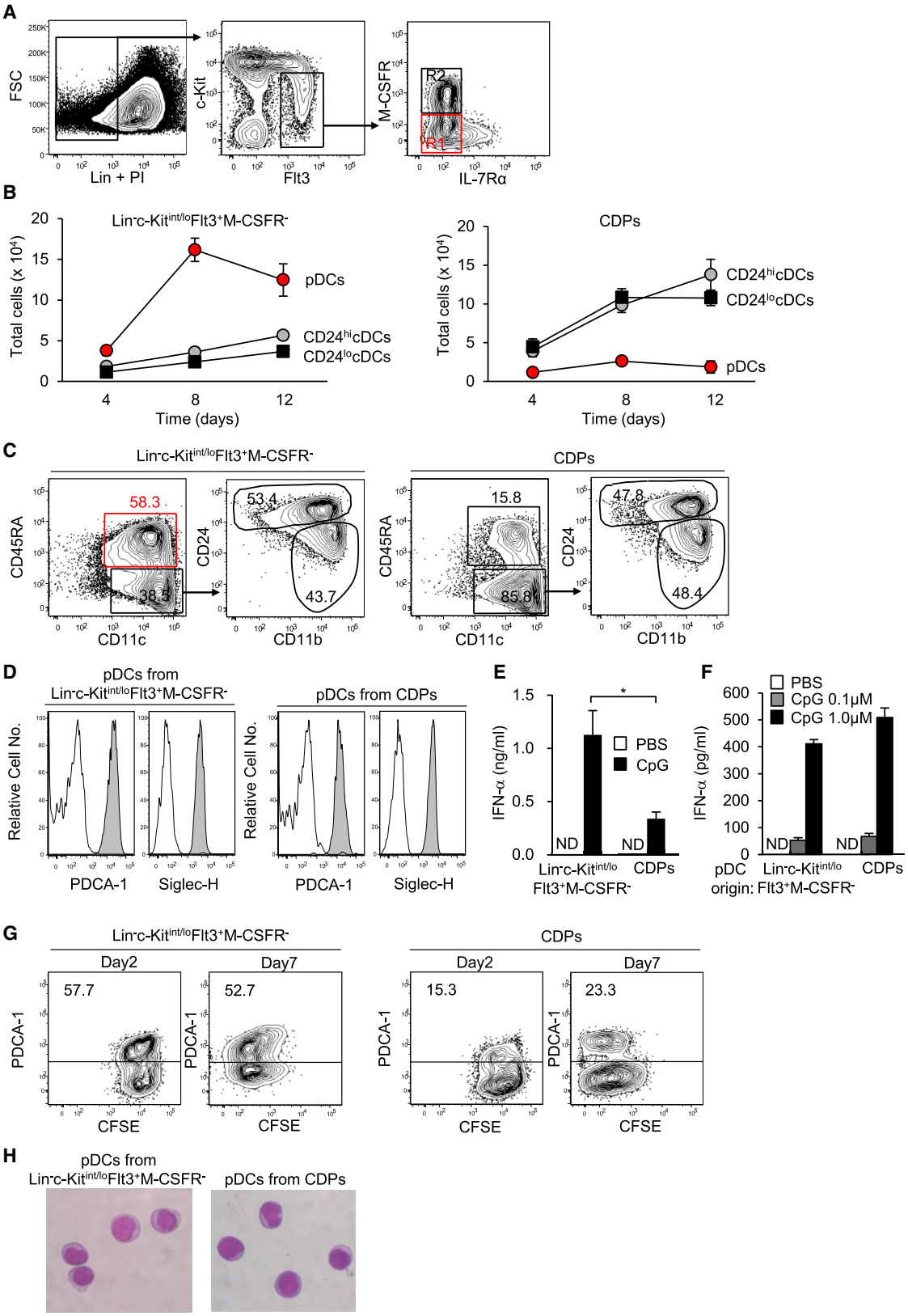

(legend on next page)

RESULTS

Identification of M-CSFR$^-$ DC Progenitors

Because the MDPs and CDPs express M-CSFR, we initially examined whether DC developmental potential was exclusive to the M-CSFR$^+$ fraction of Lin$^-$ BM cells (Figure S1 available online). Lin$^-$ BM cells were divided into four populations in terms of their c-Kit and M-CSFR expression: c-Kit^{hi}M-CSFR$^-$ (R1), c-Kit$^+$M-CSFR$^+$ (R2), c-Kit$^{int/lo}$M-CSFR$^+$ (R3), and c-Kit$^{int/lo}$M-CSFR$^-$ (R4) cells (Figure S1A). R1 contained HSCs, multipotent progenitors (MPPs), and myeloid progenitors (MPs), and R2–R4 included MDPs (R2), CDPs (R3), and B cell progenitors (R4), respectively. In the presence of M-CSF, about 50% of R2 and a few percent of R1 and R3 gave rise to macrophage colonies, but R4 did not give rise to any macrophage colonies (Figure S1B).

To examine the DC differentiation potential of each fraction, we cultured the cells ex vivo in the presence of Flt3L for 8 days. Not only the Lin$^-$M-CSFR$^+$ fractions (R2 and R3), which include the MDPs and CDPs (Fogg et al., 2006; Onai et al., 2007; Naik et al., 2007), but also the Lin$^-$M-CSFR$^-$ fractions (R1 and R4) showed DC differentiation potential (Figures S1C and S1D). Among the latter fractions, we expected the c-Kit^{hi}M-CSFR$^-$ cells (R1) to give rise to DCs, because this population contains the HSCs, MPPs, and MPs. The development of DCs from c-Kit$^{int/lo}$M-CSFR$^-$ (R4) cells was unexpected, but these cells had a relatively stronger pDC differentiation potential (Figures S1C and S1D). Because only Lin$^-$Flt3$^+$ cells have DC differentiation potential (D'Amico and Wu, 2003; Karsunky et al., 2003), we focused on Lin$^-$c-Kit$^{int/lo}$Flt3$^+$M-CSFR$^-$ cells as a likely population for the pDC precursors; we also excluded the interleukin-7 receptor α chain-positive (IL-7Rα$^+$) cells from the Lin$^-$c-Kit$^{int/lo}$Flt3$^+$M-CSFR$^-$ fraction (hereafter, Lin$^-$c-Kit$^{int/lo}$Flt3$^+$M-CSFR$^-$ cells), because this population contains B cell progenitors (Figure 1A; Onai et al., 2007). The proportion of Lin$^-$c-Kit$^{int/lo}$Flt3$^+$M-CSFR$^-$ cells was 0.1% in the whole BM cells and the ratio of Lin$^-$c-Kit$^{int/lo}$Flt3$^+$M-CSFR$^-$ cells (R1) and CDPs (R2) was 1:1 (Figure 1A).

To evaluate the DC developmental potential of the Lin$^-$c-Kit$^{int/lo}$Flt3$^+$M-CSFR$^-$ cells in comparison with CDPs ex vivo, we cultured 2 × 10^4 Lin$^-$c-Kit$^{int/lo}$Flt3$^+$M-CSFR$^-$ cells and CDPs in Flt3L-supplemented medium for 4, 8, and 12 days (Figure 1B). On day 8, when the number of pDCs reached its peak, the Lin$^-$c-Kit$^{int/lo}$Flt3$^+$M-CSFR$^-$ cells gave rise exclusively to DCs, and the majority of their progeny were pDCs (CD45RA$^+$CD11c^{int}); the rest were cDCs (CD45RA$^-$CD11c$^+$) containing both the CD11b^{lo}CD24^{hi} and CD11b^{hi}CD24^{lo} subpopulations (Figures 1B, left and 1C, left). As reported previously (Onai et al., 2007; Naik et al., 2007), CDPs gave rise to a large number of cDCs and a few pDCs (Figures 1B, right and 1C, right). On day 8, the absolute number of pDCs generated from Lin$^-$c-Kit$^{int/lo}$Flt3$^+$M-CSFR$^-$ cells was 6–8 times higher than that from CDPs. However, CDPs produced 3- to 4.5-fold more cDC subsets (Figure 1B). The CD45RA$^+$CD11c^{int} cells derived from Lin$^-$c-Kit$^{int/lo}$Flt3$^+$M-CSFR$^-$ cells and CDPs expressed plasmacytoid dendritic cell antigen-1 (PDCA-1) and sialic acid binding Ig-like lectin (Siglec)-H, confirming that they were genuine pDCs (Figure 1D). As expected from the abundant pDCs, the progenies of Lin$^-$c-Kit$^{int/lo}$Flt3$^+$M-CSFR$^-$ cells produced higher amounts of IFN-α than did those of CDPs after CpG stimulation (Figure 1E). Indeed, the same numbers of pDCs derived from Lin$^-$c-Kit$^{int/lo}$Flt3$^+$M-CSFR$^-$ cells and CDPs produced IFN-α at comparable amounts upon CpG stimulation (Figures 1F). The Lin$^-$c-Kit$^{int/lo}$Flt3$^+$M-CSFR$^-$ cells and CDPs showed similar proliferative potential ex vivo (Figure 1G), and the pDCs derived from the Lin$^-$c-Kit$^{int/lo}$Flt3$^+$M-CSFR$^-$ cells had a typical pDC morphology (Figures 1H). From these results, we concluded that Lin$^-$c-Kit$^{int/lo}$Flt3$^+$M-CSFR$^-$ cells are DC-committed progenitors with prominent pDC differentiation potential (hereafter, M-CSFR$^-$ DC progenitors).

Under the same culture conditions, 1 of 8.6 M-CSFR$^-$ DC progenitors (Figure 2A) and 1 of 7.1 CDPs (Figure 2B) gave rise to CD11c$^+$ cells as estimated by limiting-dilution analysis. That is, 43 out of 183 single-sorted M-CSFR$^-$ DC progenitors gave rise to CD11c$^+$ cells, which included 22 clones generating only pDCs, 12 generating only cDCs, and 9 generating both pDCs and cDCs (Figure 2C). In the case of cDC-only colonies, some contained both CD11b^{hi}CD24^{lo} and CD11b^{lo}CD24^{hi} subpopulations, and some contained only one of them (Figure 2D). In the case of colonies that give rise to both cDCs and pDCs, the ratio of pDCs to cDCs varied (Figure 2E). The results of limiting-dilution analysis of M-CSFR$^-$ DC progenitors (Figure 2F and CDPs (Figure 2G) were summarized as Venn diagrams, showing that

Figure 1. Identification of M-CSFR$^-$ DC Progenitors

(A) Flow cytometric sorting of BM Lin$^-$ cells (left), those expressing Lin$^-$c-Kit$^{int/lo}$Flt3$^+$ (middle), and, of them, those expressing M-CSFR and IL-7Rα (right). Boxed areas: R1, Lin$^-$c-Kit$^{int/lo}$Flt3$^+$M-CSFR$^-$IL-7Rα$^-$; R2, CDPs (Lin$^-$c-Kit$^{int/lo}$Flt3$^+$M-CSFR$^+$).

(B–E) Ex vivo DC differentiation from sorted Lin$^-$c-Kit$^{int/lo}$Flt3$^+$M-CSFR$^-$IL-7Rα$^-$ cells and CDPs.

(B) Cells (2 × 10^4) were cultured in the presence of human Flt3L-Ig (100 ng/ml) and absolute numbers of pDC (CD45RA$^+$CD11c^{int}) and cDC (CD24^{hi} cDCs and CD24^{lo} cDCs) subpopulations on day 4, 8, and 12 of culture.

(C) Flow cytometric profiles of the DC subsets.

(D) PDCA-1 or Siglec-H expression (shaded) and corresponding isotype controls (open) on pDCs.

(E) IFN-α production (1 μM CpG for 24 hr) on day 8 of culture.

(F) On day 8 of culture, pDCs derived from Lin$^-$c-Kit$^{int/lo}$Flt3$^+$M-CSFR$^-$IL-7Rα$^-$ cells and CDPs were stimulated with CpG for 24 hr, and IFN-α activity in the culture supernatants was evaluated by ELISA.

ND, not detected. Means ± SEM are shown. n = 8 from five (A–D) or three (E, F) independent experiments.

(G) Division-coupled differentiation into pDCs from Lin$^-$c-Kit$^{int/lo}$Flt3$^+$M-CSFR$^-$IL-7Rα$^-$ cells (left) and CDPs (right). DC progenitors were labeled with CFSE and cultured in the presence of hFlt3L-Ig (100 ng/ml) for 2 days and 7 days.

(H) May-Grünwald-Giemsa staining of sorted pDCs derived from Lin$^-$c-Kit$^{int/lo}$Flt3$^+$M-CSFR$^-$IL-7Rα$^-$ cells (left) and CDPs (right). Original magnification, ×400. Data are representative of three independent experiments.

See also Figure S1.

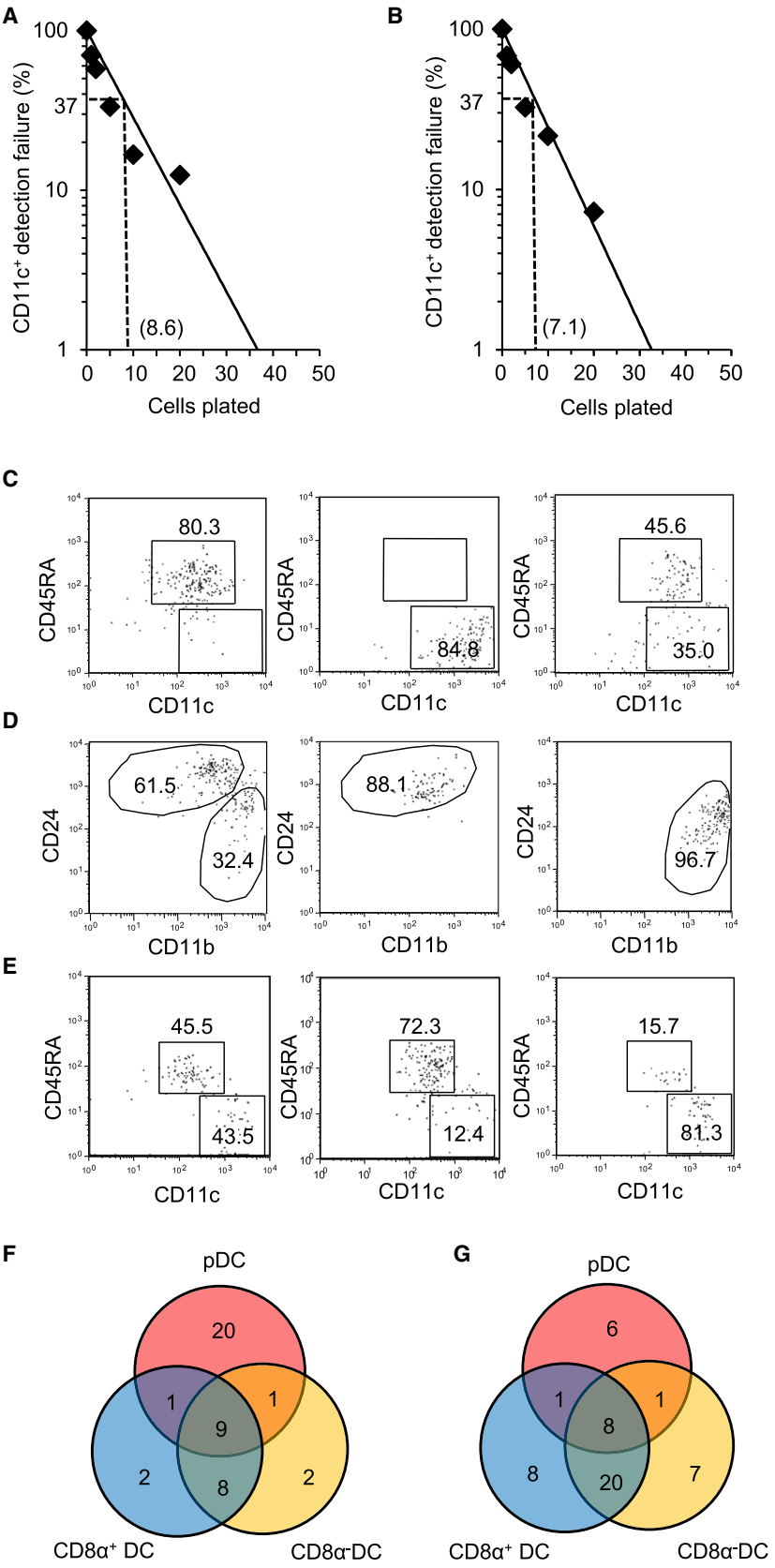

Figure 2. Limiting Dilution Analysis of M-CSFR$^-$ DC Progenitors

(A and B) Limiting dilution analysis of M-CSFR$^-$ DC progenitors (A) and CDPs (B). Cells were cultured for 12 days with Ac6 stromal cells and hFlt3L-Ig (100 ng/ml); each well was analyzed for CD11c$^+$ cells. Horizontal axis, number of plated cells. Dotted line, 37% negative "readout" showing the predicted frequency of CD11c$^+$ progenitor cells in parentheses. Statistics details are described in Experimental Procedures.

(C) Clonal analysis of M-CSFR$^-$ DC progenitors. Single progenitors gave rise to pDCs (left), cDCs (middle), or both (right).

(D) Subsets of cDCs defined as in Figure 1C.

(E) Single bipotential progenitors gave rise to both pDCs and cDCs. Some clones gave rise to comparable numbers of pDCs and cDCs (left), some clones gave rise to a large number of pDCs and some cDCs (middle), and other clones gave rise to some pDCs and many cDCs (right). Data are representative of three independent experiments.

(F and G) Venn diagrams of the progenies of single M-CSFR$^-$ DC progenitors (F) or CDPs (G) sorted and plated at a density of 1 cell per well in 96-well plates (for a total of 182 wells) on irradiated Ac6 stromal cells in human Flt3L-Ig-supplemented media. Values represent the number of wells on day 12 with cells of the indicated type. Data are combined from three independent experiments.

See also Figure S2.

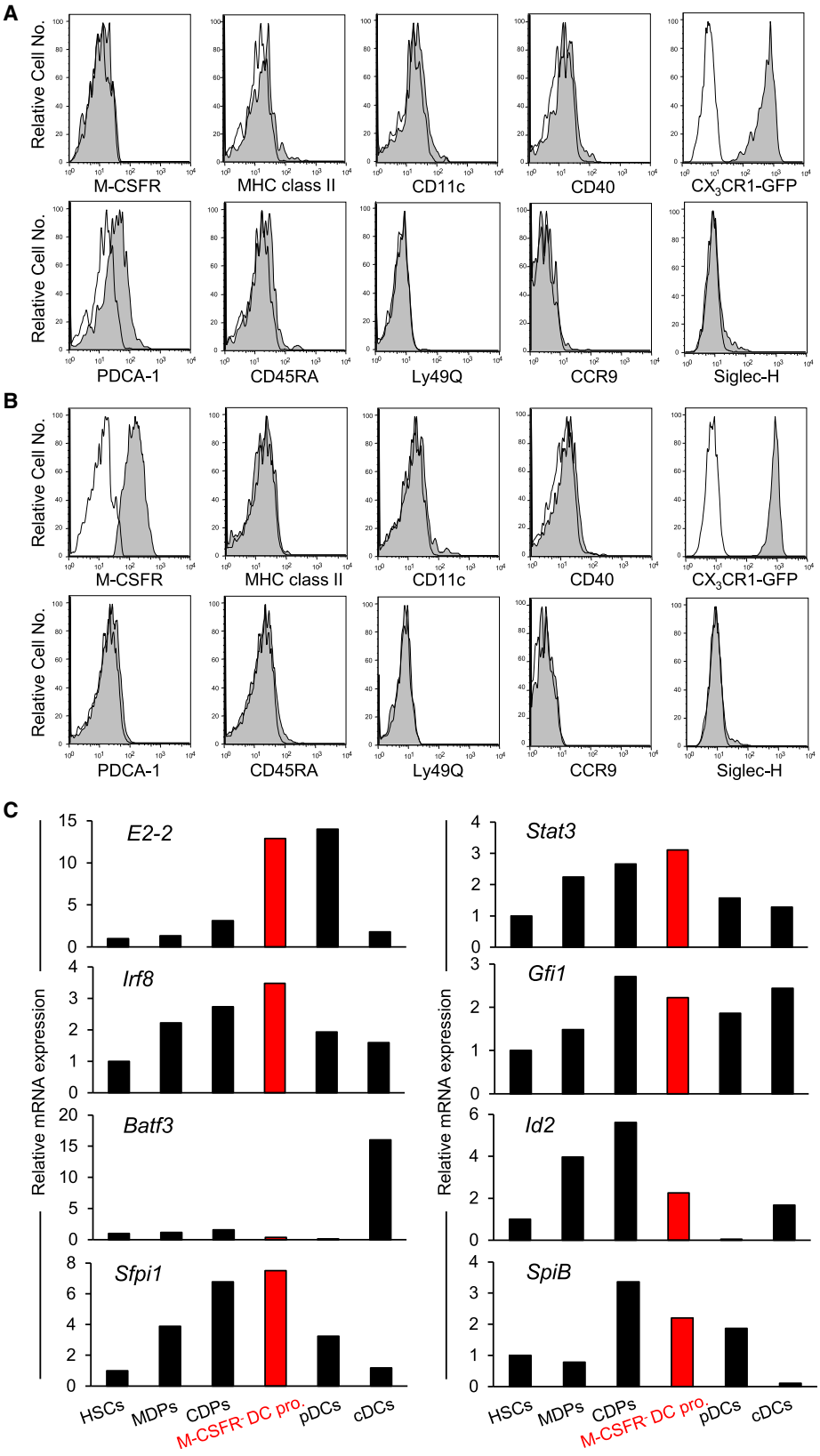

(legend on next page)

M-CSFR$^-$ DC progenitors contain more clones that give rise to pDCs.

To further ensure DC-committed differentiation potential of M-CSFR$^-$ DC progenitors, we examined the myelo-erythroid and B cell differentiation potential of M-CSFR$^-$ DC progenitors by using ex vivo assays for colony-forming units (CFU) (Figures S2A–S2C). For comparison, Lin$^-$c-Kit^{hi}Sca-1$^+$ cells, which are a mixture of HSCs and MPPs, were included. As reported previously (Fogg et al., 2006; Auffray et al., 2009; Liu et al., 2009; Onai et al., 2007; Naik et al., 2007), MDPs contained colony-forming activities for myeloid lineages, resulting in colonies of granulocytes and macrophages or macrophages alone, but less than 3% of the CDPs produced myeloid colonies. In contrast, M-CSFR$^-$ DC progenitors contained few macrophage CFU and completely lacked CFU for other myeloid lineages (Figure S2A). Furthermore, compared with MDPs, CDPs and M-CSFR$^-$ DC progenitors produced few macrophage colonies, and neither of them produced pre-B cells (Figures S2B and S2C). Therefore, we concluded that M-CSFR$^-$ DC progenitors have minimal myeloid differentiation potential and lack erythroid and pre-B cell differentiation potential.

M-CSFR$^-$ DC Progenitors Highly Express *E2-2*

We further characterized in detail the molecular phenotypes of the M-CSFR$^-$ DC progenitors. First we examined their expression of cell surface molecules and found that they were positive for CX_3CR1, expressed PDCA-1 at minimal amounts, and were negative for M-CSFR, MHC class II, CD11c, CD40, CD45RA, Ly49Q, CCR9, and Siglec-H (Figure 3A). In this context, CDPs expressed M-CSFR but never expressed PDCA-1 (Figure 3B). In addition, DNA microarray analysis revealed that the M-CSFR$^-$ DC progenitors did not distinctly express other surface markers including receptors for cytokines and chemokines (Table S1). Several transcription factors critically regulate DC development (Merad and Manz, 2009; Watowich and Liu, 2010; Belz and Nutt, 2012): the basic helix-loop-helix transcription factor E2-2 specifically controls pDC development (Nagasawa et al., 2008; Cisse et al., 2008; Ghosh et al., 2010), interferon regulatory factor 8 (IRF) controls the development of pDCs and certain cDC subsets (Schiavoni et al., 2002, 2004; Aliberti et al., 2003; Tsujimura et al., 2003), Batf3 is required for CD8α^+ and CD103$^+$ cDC development (Hildner et al., 2008; Edelson et al., 2010), and PU.1, encoded by *Sfpi1*, seems to regulate both cDC and pDC development (Anderson et al., 2000; Guerriero et al., 2000; Onai et al., 2006). Other factors controlling DC development include STAT3, Gfi-1, Id2, and SpiB. We examined the expression profiles of these DC development-associated genes in the M-CSFR$^-$ DC progenitors and in HSCs, MDPs, CDPs, pDCs, and cDCs (Figure 3C). Importantly, the M-CSFR$^-$ DC progenitors expressed the highest amounts of *E2-2* among those tested, consistent with their prominent pDC differentiation potential. They also expressed critical DC lineage-associated genes, such as *Irf8*, *Sfpi1*, *Stat3*, *Gfi1*, and *SpiB* at amounts comparable to CDPs, and *Id2* at lower amounts than the other DC progenitors, confirming their DC developmental potential. In contrast, *Batf3* expression in the M-CSFR$^-$ DC progenitors was negligible. These results indicated that the molecular phenotypes of the M-CSFR$^-$ DC progenitors are suitable for DC progenitors and the highest amounts of *E2-2* expression is consistent with their prominent pDC differentiation potential.

In Vivo Prominent pDC Differentiation Potential of M-CSFR$^-$ DC Progenitors

To evaluate the in vivo differentiation potential of the M-CSFR$^-$ DC progenitors, 5 × 10^4 M-CSFR$^-$ DC progenitors or CDPs from B6 mice (CD45.1$^-$CD45.2$^+$) were injected into irradiated B6.SJL mice (CD45.1$^+$CD45.2$^-$) (Figure 4). In line with our ex vivo findings, the M-CSFR$^-$ DC progenitors gave rise exclusively to DCs and not to lineages including T, B, and NK cells, or erythrocytes in the spleen and BM of the progenitor-injected mice (Figures 4A and 4B). Furthermore, 10 days after the transplantation, when the number of progeny cells peaked (Figure 4C), most of the M-CSFR$^-$ DC progenitors' progenies were pDCs (CD45RA$^+$CD11c^{int}) in these organs, which expressed additional pDC markers, including PDCA-1 and Siglec-H (Figures 4A and 4B). Compared with CDPs, the M-CSFR$^-$ DC progenitors gave rise to 5–6 times more pDCs, but only 1/3 the number of cDCs (Figure 4D). In addition, the M-CSFR$^-$ DC progenitor-derived pDCs and cDCs expressed normal amounts of Toll-like receptor 7 (TLR7) and TLR9 and of TLR2 and TLR4, respectively (Figures 4E and S3A); the pDCs were capable of producing robust IFN-α in response to CpG stimulation ex vivo (Figure 4F); and the cDCs effectively induced T cell proliferation in allogeneic mixed lymphocyte reactions (MLRs) (Figure S3B). To further demonstrate the biological relevance of the M-CSFR$^-$ DC progenitors in vivo, the M-CSFR$^-$ DC progenitors, MDPs, and CDPs were transplanted into irradiated mice. Ten days after transplantation, CpG DNA$^+$DOTAP was intravenously injected, and the serum concentration of IFN-α was examined. Consistent with the prominent pDC developmental potential of the M-CSFR$^-$ DC progenitors, the mice that received these cells produced a significantly higher amount of IFN-α than those transplanted with MDPs or CDPs (Figure 4G). Because the LNs became too small to analyze after irradiation, we also transplanted the M-CSFR$^-$ DC progenitors into nonirradiated recipients and noted that they gave rise to a large number of pDCs in the spleen, LNs, and BM (Figures S3C–S3G). Of note, the progenies were mostly pDCs in the BM, which is consistent with a previous report showing that pDCs are abundantly present in the BM under steady-state conditions (Zhang et al., 2006). In addition, the M-CSFR$^-$ DC progenitor-derived pDCs contained a larger number of CCR9$^-$ subpopulation in the BM than those in the spleen (Figures S3E). To further examine whether DC progenitors give rise to pDCs through CCR9$^-$ intermediate precursors (Schlitzer et al., 2011), we cultured 2 × 10^4 M-CSFR$^-$ DC progenitors in Flt3L-supplemented medium for 2 or 4 days (Figure S3H). The

Figure 3. Characterization of M-CSFR$^-$ DC Progenitors

(A and B) Histograms showing surface markers of M-CSFR$^-$ DC progenitors (A) and CDPs (B). Shaded areas, indicated molecules; open areas, corresponding isotype controls.

(C) RNAs for DC lineage-associated genes were analyzed by qPCR in HSCs, MDPs, CDPs, M-CSFR$^-$ DC progenitors, pDCs, and cDCs.

Data are representative of three independent experiments. See also Table S1.

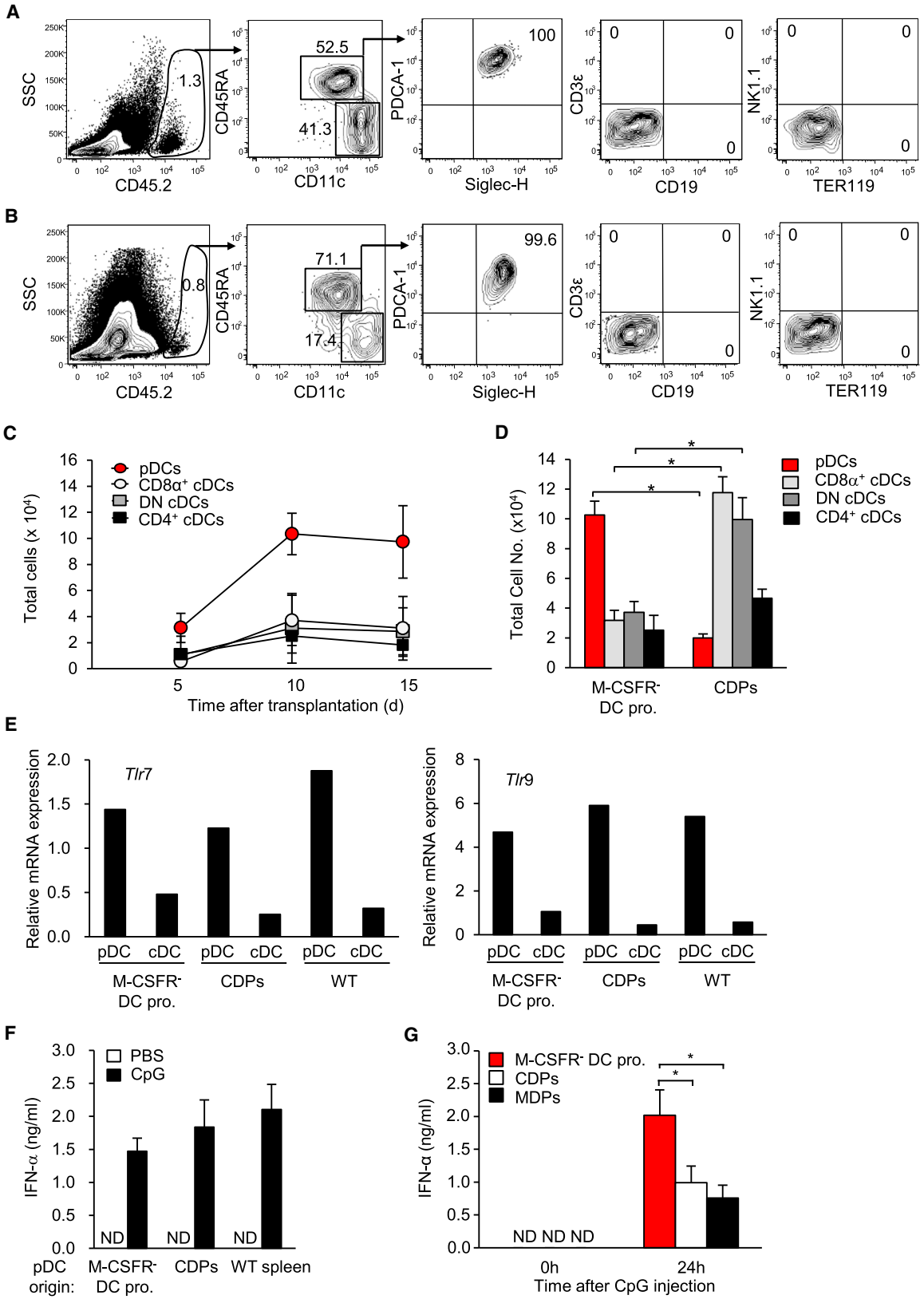

(legend on next page)

M-CSFR$^-$ DC progenitors clearly expressed PDCA-1 as early as day 2 (data not shown) and started to express CCR9 on day 2. Its amount had increased on day 4, showing that CCR9$^-$ intermediate precursors give rise to pDCs (Figure S3H). These results collectively indicated that M-CSFR$^-$ DC progenitors have excellent pDC differentiation potential in vivo.

Rag1$^+$ pDCs Are Derived from the M-CSFR$^-$ DC Progenitors

Although pDCs are heterogeneous and 30%–40% of them express Rag1 (Pelayo et al., 2005), CDPs are entirely Rag1 negative, implying the presence of other DC progenitors that generate Rag1-positive pDCs (Reizis, 2010). To examine whether the M-CSFR$^-$ DC progenitors give rise to both Rag1-positive and Rag1-negative pDCs in vivo, 5 × 10^4 M-CSFR$^-$ DC progenitors or CDPs of *Rag1*$^{gfp/+}$ mice (CD45.1$^-$CD45.2$^+$), which express enhanced green fluorescent protein (EGFP) under the endogenous *Rag1* promoter (Kuwata et al., 1999), were transplanted into irradiated B6.SJL mice (CD45.1$^+$ CD45.2$^-$) (Figure 5). Of note, the majority of the CDPs (99.9%) and the M-CSFR$^-$ DC progenitors (97.9%) did not express Rag1 (Figure 5A). Consistent with these results, the D_H-J_H rearrangement was not detectable in the M-CSFR$^-$ DC progenitors or CDPs, although it was detected in these progenitor-derived pDCs (Figure S4). Ten days after the transplantation, M-CSFR$^-$ DC progenitors had given rise to a 2:1 ratio of Rag1-negative to Rag1-positive pDCs, whereas no Rag1-positive cDCs were detected in vivo (Figures 5B and 5F). Both pDC subsets expressed CCR9, although a small fraction of the Rag1-negative pDCs did not (Figure 5C). In contrast, most of the CDP-derived pDCs were Rag1 negative (Figures 5D and 5F) and, regardless of the Rag1 expression, the majority of pDCs expressed CCR9 (Figure 5E). These results suggested that both Rag1-negative and -positive pDCs are mostly derived from the M-CSFR$^-$ DC progenitors in vivo. No Rag1-positive cDCs were derived from either the CDPs or the M-CSFR$^-$ DC progenitors (Figure 5G).

Relationship between the M-CSFR$^-$ DC Progenitors and CDPs

Finally, the relationship between the M-CSFR$^-$ DC progenitors and CDPs was examined. Based on the findings that the M-CSFR$^-$ DC progenitors do not express M-CSFR, whereas MDPs and CDPs do express it (Figure 3A), that Flt3L and M-CSF promote pDC development from CDPs (Onai et al., 2007), and that Flt3L and thrombopoietin (TPO) promote pDC development from human CD34$^+$ cells (Chen et al., 2004), we cultured M-CSFR$^-$ DC progenitors, side by side with CDPs and MDPs, in the presence of Flt3L alone or Flt3L and M-CSF and/or TPO for 8 days. Compared with Flt3L alone, Flt3L together with TPO further enhanced pDC differentiation from the M-CSFR$^-$ DC progenitors, and Flt3L together with M-CSF and/or TPO significantly enhanced the differentiation of pDCs, but not cDCs, from CDPs, and, to a lesser extent, from MDPs (Figures 6A, 6B, S5A, and S5B). Of note, Flt3L induced the expression of Mpl, a receptor for TPO, on the DC progenitors (Figure 6C), allowing them to respond to TPO. Importantly, under this culture condition, the progenitors' *E2-2* mRNA expression was upregulated (Figures 6D, left, and S5C), whereas their M-CSFR expression was downregulated although the amount of M-CSFR downregulation by Flt3L and TPO was partial (Figures 6E and S5D), resulting in the M-CSFR$^-$ DC progenitor-like phenotype. Of note, when both M-CSF and TPO were added together with Flt3L, their enhancing effects on pDC differentiation were not additive. Consistent with these results, 3 days after an intra-BM transfer of DC progenitors, the M-CSFR$^-$ DC progenitors had maintained their surface phenotype, whereas the c-Kit and M-CSFR expression on CDPs and on nearly half of the MDPs was downregulated (Figure S5E). These results suggested that the M-CSFR$^-$ DC progenitors might be derived from CDPs that were stimulated with cytokines that upregulate E2-2 expression, i.e., M-CSF and TPO.

In addition, an upstream Flt3$^+$ progenitor might generate both CDPs and the M-CSFR$^-$ DC progenitors. To test this possibility, we focused on lymphoid-primed MPPs (LMPPs, also known as MPP4), which are Lin$^-$c-Kit$^+$Sca-1$^+$CD34$^+$Flt3$^+$ and lack megakaryocyte and erythroid potential (Adolfsson et al., 2005; Wilson et al., 2008), for the following reasons. First, megakaryocyte and erythroid progenitors (MEPs) do not have DC developmental potential (Onai et al., 2006). Second, granulocyte and monocyte progenitors (GMPs) showed a very low pDC developmental potential (data not shown). We transplanted CFSE-labeled LMPPs (CD45.1$^-$CD45.2$^+$) directly into the BM of nonirradiated B6.SJL mice (CD45.1$^+$CD45.2$^-$). Soon after the LMPPs divided once, we identified daughter cells showing the surface phenotype of the M-CSFR$^-$ DC progenitors (Figure 7A) that retained their unique DC differentiation potential (Figures 7B and 7C). Interestingly, this was also the case for MDPs and CDPs (Figures 7A–7C). In this context, our data include the previously proposed differentiation pathways, i.e., the differentiation of GMPs and MDPs into CDPs (Liu et al., 2009). On the basis of these findings, we propose a new model for DC development, in which

Figure 4. In Vivo Differentiation Potential of M-CSFR$^-$ DC Progenitors

(A and B) Flow cytometric profile of the spleen (A) and BM (B) 10 days after i.v. transplantation of 5 × 10^4 double-sorted M-CSFR$^-$ DC progenitors from B6 mice (CD45.2$^+$) into irradiated B6.SJL mice (CD45.1$^+$). Progenies were stained for CD11c, CD45RA, PDCA-1, Siglec-H, CD3ε, CD19, NK1.1, and TER119.

(C and D) Absolute cell numbers of DC subsets in splenic progenies from M-CSFR$^-$ DC progenitors at the indicated time points (C) and from M-CSFR$^-$ DC progenitors or CDPs at day 10 (D).

(E) Splenic pDC and cDC progenies were sorted, and the expression levels of *Tlr7* and *Tlr9* were analyzed by qPCR. Data are representative of two independent experiments.

(F) Ten days after transplantation, M-CSFR$^-$ DC progenitor (pro.)-derived pDCs were sorted from the spleen and stimulated with 1 μM CpG for 24 hr, and the IFN-α concentrations in the culture supernatants were determined by ELISA.

(G) Sorted M-CSFR$^-$ DC progenitor, CDPs, and MDPs were transplanted into lethally irradiated B6.SJL mice with rescue bone marrow. Ten days after transplantation, CpG + DOTAP was intravenously injected, and 24 hr later the serum IFN-α concentration was determined by ELISA. Data are representative of three independent experiments. ND, not detected.

Error bars in (C), (D), (F), and (G) show the mean ± SEM. *$p < 0.01$. See also Figure S3.

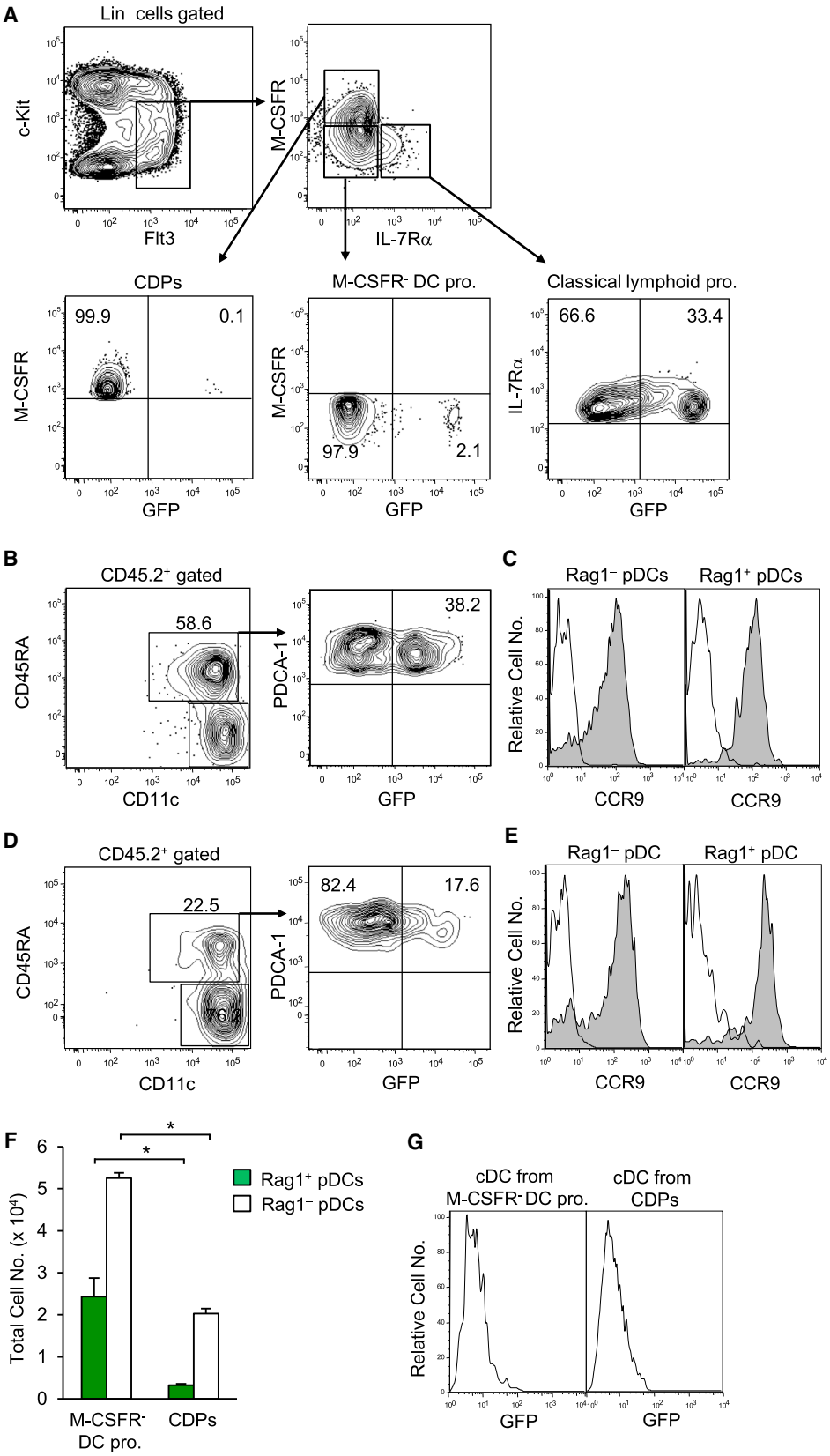

(legend on next page)

M-CSFR$^-$ DC progenitors are derived from either CDPs or LMPPs (Figure S6).

DISCUSSION

Our findings extend the previous knowledge that DC-committed progenitors are confined to the Lin$^-$Flt3$^+$ fraction (D'Amico and Wu, 2003; Karsunky et al., 2003) to show that DC-committed progenitors belong to the Lin$^-$c-Kit$^{int/lo}$Flt3$^+$IL-7Rα^- fraction and that M-CSFR expression does not determine their presence. Thus, we propose that DC-committed progenitors consist of the M-CSFR$^-$ DC progenitors and CDPs, with the former probably arising downstream of the latter or LMPPs.

One could argue against the proposed relationship between the M-CSFR$^-$ DC progenitors and CDPs. When CDPs were transferred in vivo, they gave rise to large numbers of cDCs and few pDCs, seemingly arguing against the ex vivo findings that CDPs stimulated with M-CSF and/or TPO become the M-CSFR$^-$ DC progenitor-like cells with prominent pDC differentiation potential. In this context, progenitor transfer experiments might be appropriate to demonstrate each progenitor's own DC differentiation potential. However, it is uncertain whether progenitors transferred in vivo migrate to and settle in the "progenitor niche" where they are exposed to the appropriate cytokines and other ligands necessary for the conversion from CDPs to the M-CSFR$^-$ DC progenitors. Therefore, such transfer experiments have some technical limitations and might not demonstrate the physiological fate of the progenitor cells. In addition, our results showed that LMPPs are a possible upstream progenitor for both CDPs and the M-CSFR$^-$ DC progenitors.

Besides these two DC-committed progenitors, other DC-committed progenitor candidates are unlikely to be present in the Lin$^-$Flt3$^+$ fraction, because the Lin$^-$c-Kit$^{hi/+}$Flt3$^+$ population contains short-term HSCs, multipotent progenitors, earlier progenitors upstream of MDPs, and MDPs, and the rest of the Lin$^-$c-Kit$^{int/lo}$Flt3$^+$ cells are Lin$^-$c-Kit$^{int/lo}$Flt3$^+$M-CSFR$^-$IL-7Rα^+, with B cell differentiation potential. Based on previous findings and our results, we propose the following scenario for DC development. DC lineage commitment occurs in the Lin$^-$c-Kit$^{int/lo}$Flt3$^+$IL-7Rα^- fraction upon receiving the Flt3 signal, which plays a nonredundant role in DC development (McKenna et al., 2000; Onai et al., 2006; Waskow et al., 2008). Then, the cells receiving a second signal via M-CSFR or Mpl, a receptor for TPO, upregulate E2-2 and reciprocally downregulate M-CSFR, further committing them to the pDC lineage.

In this context, although M-CSF can induce pDCs and cDCs ex vivo and in vivo independently of Flt3L, the numbers of pDCs and cDCs generated are much reduced compared with the effect of M-CSF in Flt3L-sufficient conditions (Fancke et al., 2008), suggesting that the Flt3 signal is prerequisite for M-CSF to optimally influence DC development. In addition, M-CSF and TPO (and probably even other cytokines) function redundantly to upregulate E2-2. Therefore, mice lacking a single cytokine or its receptor gene may be unlikely to show impaired pDC development. In contrast to the M-CSF-induced downregulation of M-CSFR, the mechanism of TPO-induced M-CSFR downregulation remains unknown. The promoter region of M-CSFR contains an E-box, which is an E2-2-binding site (Ovchinnikov et al., 2010), implying that TPO-induced E2-2 might downregulate M-CSFR. In addition, DNA microarray analysis revealed that, except for M-CSFR, the expression amounts of receptors for known cytokines and ligands were comparable between the M-CSFR$^-$ DC progenitors and CDPs The microenvironments in the BM, i.e., the cells that physiologically secrete M-CSF and TPO, by which CDPs acquire E2-2 and the distinct set of transcriptional gene expressions associated with the pDC developmental potential, remains an important issue to be addressed.

pDCs are heterogenous and can be divided into subpopulations based on the expression of Rag1 and CCR9 (Pelayo et al., 2005; Schlitzer et al., 2011). Because CDPs are uniformly negative for Rag1, the possibility of a partial lymphoid contribution to pDC development or the presence of some other source of pDCs that expresses Rag1 has been suggested (Reizis, 2010). The M-CSFR$^-$ DC progenitors described here gave rise to both Rag1-negative and -positive pDCs in vivo. In addition, consistent with a recent report identifying PDCA-1$^+$CCR9$^-$ cells as a pDC precursor (Schlitzer et al., 2011), the M-CSFR$^-$ DC progenitors gave rise to PDCA-1$^+$CCR9$^+$ pDCs via the PDCA-1$^+$CCR9$^-$ precursor stage. Interestingly, the PDCA-1$^+$CCR9$^-$ cells largely give rise to pDCs in the BM and liver, but they give rise to both pDCs and cDCs in other peripheral lymphoid organs, implying that their DC developmental potential is affected by tissue-derived cytokines that regulate the amounts of *E2-2* and *Id2* expression (Schlitzer et al., 2012).

The M-CSFR$^-$ DC progenitors gave rise to predominantly pDCs and some cDCs, indicating that the identity of the progenitors hasn't been definitively confirmed. In this context, because they express only low amounts of PDCA-1, it is technically impossible to clearly sort PDCA-1$^-$ and PDCA-1^{lo} cells. Furthermore, cell surface staining for more than 20 different markers including M-CSFR, MHC class II, CD11c, CD40, CX_3CR1, CD45RA, Ly49Q, CCR9, and Siglec-H and DNA microarray analysis revealed that the M-CSFR$^-$ DC progenitors do not distinctly express other surface markers, suggesting that the ability to identify progenitors with a unique pDC differentiation potential on the basis of surface markers is limited. Instead, because they express the highest levels of *E2-2* but still give rise to some cDCs, it is likely that the M-CSFR$^-$ DC progenitors represent a mixture of cells, the majority of which express *E2-2* and the rest of which express little or no *E2-2* and probably contain

Figure 5. M-CSFR$^-$ DC Progenitors as a Source of pDC Subsets

(A) Flow cytometric analysis of CDPs, M-CSFR$^-$ DC progenitor, and classical lymphoid progenitors (Lin$^-$c-Kit$^{int/lo}$Flt3$^+$M-CSFR$^-$IL-7Rα^+) for Rag1 expression. (B–G) Flow cytometric profile (B–E, G) and absolute numbers (F) of spleen progeny 10 days after i.v. transplantation of 5 × 10^4 sorted M-CSFR$^-$ DC progenitors (B, C) and CDPs (D, E) from *Rag1*$^{gfp/+}$ mice (CD45.2$^+$) into irradiated B6.SJL mice (CD45.1$^+$). The resulting pDCs were further analyzed for GFP (B, D) and CCR9 (C, E) amounts. The resulting cDCs were also analyzed for GFP amounts (G). Shaded histograms show CCR9 expression on Rag1$^-$ (left) and Rag1$^+$ (right) pDCs; open histograms represent results from corresponding isotype controls. Cell numbers are graphed in (F). Data are representative of three independent experiments. Error bars in (F) show the mean ± SEM. *$p < 0.01$.

See also Figure S4.

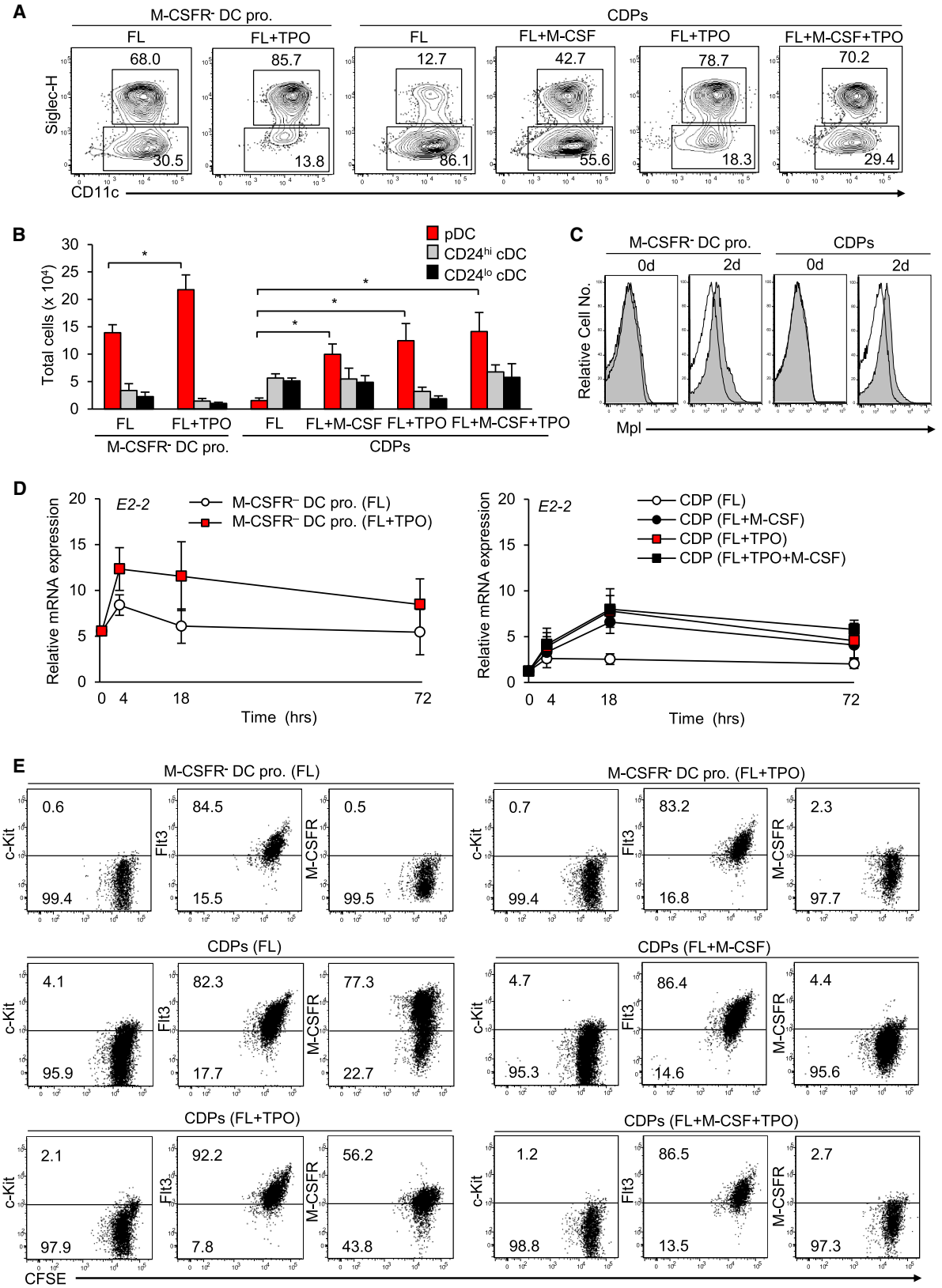

(legend on next page)

at least in part previous CDPs with retained cDC differentiation potential; the former give rise strictly to pDCs, whereas the latter give rise to cDCs. To identify progenitors with a unique pDC differentiation potential will require an *E2-2* reporter mouse. Based on our findings, we suggest redefining CDPs to include both E2-2^{lo} and E2-2^{hi} cells regardless of M-CSFR expression.

Given that pDCs contribute critically to the induction of antiviral immune responses (Banchereau and Steinman, 1998; Liu, 2005; Shortman and Naik, 2007; Geissmann et al., 2010; Swiecki and Colonna, 2010), oral tolerance (Goubier et al., 2008), and the development of autoimmune diseases (Gilliet et al., 2008; Banchereau and Pascual, 2006), our discovery of genuine pDC progenitors, which provides insight into DC differentiation pathways, may also lead to progenitor-based therapies for viral infection and autoimmune disease.

EXPERIMENTAL PROCEDURES

Mice

C57BL/6 (B6 mice, Clea), B6.*Cx$_3$cr1*$^{gfp/+}$ (Jackson) (Jung et al., 2000), B6.SJL-ptprc^a mice congenic at the CD45 locus (B6.SJL mice), and B6.*Rag1*$^{gfp/+}$ (Kuwata et al., 1999) mice were maintained in our SPF facility. All animal experiments were approved by the Institutional Animal Care Committee of Tokyo Medical and Dental University.

Cell Sorting and Flow Cytometric Analysis

BM lineage negative (Lin$^-$) cells were immunomagnetically pre-enriched with PE-Cy5-conjugated antibodies against lineage antigens including CD3ε (145-2C11), CD4 (GK1.5), CD8α (53-6.7), B220 (RA3-6B2), CD19 (MB19-1), CD11c (N418), MHC class II (I-A and I-E; M5/114.15.2), CD11b (M1/70), Gr-1 (RB6-8C5), TER119 (TER119), NK1.1 (PK136) (all from BioLegend), and anti-Cy5-MicroBeads (Miltenyi Biotec). BM Lin$^-$ cells were then stained with FITC-anti-CD34 (RAM34), PE-anti-Flt3 (A2F10.1), PE-Cy7-anti-Sca-1 (D7), APC-anti-c-Kit (ACK2), Brilliant Violet 421-anti-IL-7Rα (A7P34), and Biotin-anti-M-CSFR (AFS-98) (all from BioLegend). Secondary labeling was performed with Streptavidin-APC-eFluor 780 (eBioscience). M-CSFR$^-$ DC progenitors as well as MDPs, CDPs, and LMPPs were sorted as Lin$^-$c-Kit$^{int/lo}$ Flt3$^+$M-CSFR$^-$IL-7Rα$^-$ cells, Lin$^-$c-Kit$^+$Flt3$^+$M-CSFR$^+$ cells, Lin$^-$c-Kit$^{int/lo}$ Flt3$^+$M-CSFR$^+$ cells, and Lin$^-$c-Kit$^+$Sca-1$^+$CD34$^+$Flt3$^+$ cells, respectively, on a MoFlo instrument (Beckman Coulter) and analyzed on a FACSCanto II (BD Biosciences) in conjunction with FlowJo software (TreeStar). Antibodies against the following molecules were used for further phenotypic analysis of DC progenitors: MHC class II (I-A and I-E; M5/114.15.2), CD11c (N418), CD40 (1C10), and Siglec-H (eBio440c) (all from eBioscience), PDCA-1 (JF05-1C.2.4.1, Miltenyi Biotec), CD45RA (14.8, BD Biosciences), CCR9 (242503, R&D), Mpl (AMM2, Kyowa Hakko Kirin), and Ly49Q (NS34) (Toyama-Sorimachi et al., 2004). The cells were analyzed on a FACSCalibur or a FACSCanto II (BD Biosciences) in conjunction with FlowJo software (TreeStar).

Limiting-Dilution Analysis

Limiting-dilution assays were performed as described (Onai et al., 2007). Ac6 stromal cells were seeded at a density of 5 × 10^3 cells per well in 96-well flat-bottomed plates 1 day before starting coculture. Lin$^-$c-Kit$^{int/lo}$Flt3$^+$ M-CSFR$^-$IL-7Rα$^-$ cells were sorted and plated on irradiated Ac6 cells at a density of 100, 50, 10, 2, or 1 cells per well. Cells were cultured as described (Onai et al., 2007) and analyzed on day 12. The frequency of pDCs and/or cDCs derived from progenitors was evaluated on a FACSCanto II (BD) via "Loi de Poisson" statistics. Only wells containing more than 128 cells were considered positive. Statistics were calculated based on the mean values of each dilution step; the correlation coefficient for curve extrapolation was $r = 0.9706$.

In Vivo Reconstitution Assays

Fifty thousand double-sorted M-CSFR$^-$ DC progenitors from B6 mice (CD45.1$^-$CD45.2$^+$) were injected i.v. into lethally X-ray-irradiated (9 Gy, Faxitron) B6.SJL mice (CD45.1$^+$CD45.2$^-$). When irradiated, 2 × 10^5 recipient type whole BM cells were added to the injections. Intra-BMT was performed as described (Kushida et al., 2001). Fifty thousand double-sorted DC progenitors from B6 mice were suspended in 10 μl of PBS and carefully injected through a hole in the bone into the BM cavity of nonirradiated B6.SJL mice with a customized Ito microsyringe (Ito Corp.). Mice were killed 10 days after the reconstitution, and their splenic progenies were analyzed for the frequency of cDCs and pDCs. In some experiments, CFSE-labeled 2 × 10^5 M-CSFR$^-$ DC progenitors, CDPs, MDPs, or 1 × 10^5 MPPs were directly injected into the BM (intra-BMT) of nonirradiated B6.SJL mice. Three days after the transplantation, the BM progenies were resorted and cultured in the presence of irradiated Ac6, Flt3L, and TPO for 8 days.

Quantitative RT-PCR

Total RNA was extracted with the RNeasy Mini Kit (QIAGEN), and cDNA was synthesized with random hexamers and SuperScript III reverse transcriptase. For real-time PCR, cDNA products equivalent to the RNAs from 500 cells were amplified with a LightCycler480 SYBR Green I Master (Roche Diagnostics). The data were normalized to the amount of *gapdh* RNA expression in each sample. The primers used for real-time PCR were as follows: *E2-2* sense, 5′-TGAGATCAAATCCGACGA-3′ and antisense, 5′-CGTTATTGCTAGATCTT GACCT-3′; *Irf8* sense, 5′-AAGGGCGTGTTCGTGAAG-3′ and antisense, 5′-GGTGGCGTAGAATTGCTG-3′; *Sfpi1* sense, 5′-ATGCACGTCCTCGATA CTC-3′ and antisense, 5′-TCTCACCCTCCTCCTCATCT-3′; *Spib* sense 5′-CA CTCCCAAACTGTTCAGC-3′ and antisense, 5′-TGGGGTACGGAGCATAAG-3′; *Stat3* sense, 5′-TGGGTGGAAAAGGACATCAG-3′ and antisense, 5′-GGA ATGTGGGGGTAGAGGTA-37; *Gfi1* sense 5′-CAAGAAGGCGCACAGCTA-3′ and antisense 5′-GGGCTCCATTTTGGACTC-3′; *Batf3* sense, 5′-AGACCCA GAAGGCTGACAA-3′ and antisense, 5′-CTGCACAAAGTTCATAGGACAC-3′; *Id2* sense, 5′-CATGAACGACTGCTACTCCAA-3′ and antisense, 5′-GTGATG CAGGCTGACGATAGT-3′; and *Gapdh* sense, 5′-TCCACCACCCTGTTGCTG TA-3′ and antisense, 5′-ACCACAGTCCATGCCATCAC-3′. Primers were synthesized by Operon Biotechnologies.

DC Functional Assays

In some in vivo experiments, CpG (D-19, 5 μg) in 50 μl HBSS was mixed with 30 μl DOTAP reagent (Roche) and 20 μl HBSS for 15 min at room temperature (CpG+DOTAP). CpG+DOTAP was injected into B6.SJL mice that were lethally irradiated and transplanted with DC progenitors and the serum IFN-α was evaluated by ELISA 24 hr after the injection.

Statistical Analysis

We evaluated the statistical significance of the obtained values by the two-tailed Student's t test. A p value of <0.05 was considered significant.

Figure 6. Relationship between the M-CSFR$^-$ DC Progenitors and CDPs

Sorted M-CSFR$^-$ DC progenitors and CDPs (2 × 10^4) were cultured in the presence of hFlt3L-Ig (FL) (100 ng/ml), hFlt3L-Ig + M-CSF (20 ng/ml), hFlt3L-Ig + human TPO (20 ng/ml), or hFlt3L-Ig + M-CSF (20 ng/ml) + hTPO (20 ng/ml).

(A) Flow cytometric profiles of the DC subsets.

(B) Absolute numbers of the pDC and cDC subpopulations (CD24^{hi} cDCs and CD24^{lo} cDCs) on day 8 of culture.

(C) Expression of Mpl on DC progenitors cultured with human Flt3L-Ig for 2 days.

(D) Relative *E2-2* mRNA expression in cytokine-stimulated DC progenitors at the indicated time points during culture.

(E) DC progenitors were labeled with CFSE and cultured as indicated for 2 days.

Data are representative of three independent experiments. Error bars in (B) and (D) show the mean ± SEM. *p < 0.01. See also Figure S5.

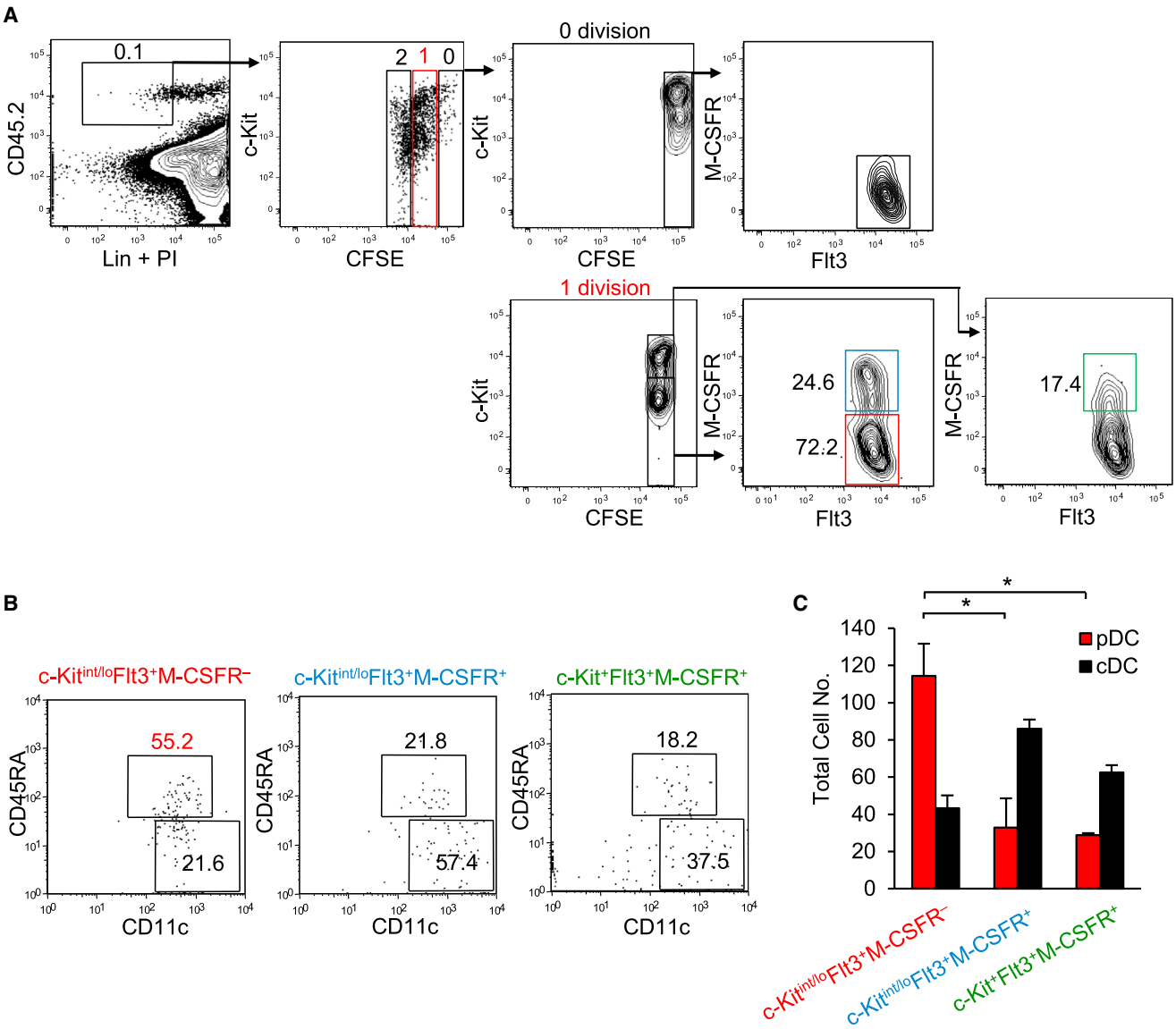

Figure 7. LMPPs Give Rise to M-CSFR⁻ DC Progenitors, CDPs, and MDPs In Vivo

Sorted and CFSE-labeled LMPPs (1 × 10^5 cells) were transplanted directly into the BM (intra-BMT) of nonirradiated B6.SJL mice.

(A) Representative flow cytometric profiles of BM progenies 3 days after intra-BMT are shown.

(B) Representative flow cytometric profiles of the progenies of sorted CFSE$^+$LMPP-derived c-Kit$^{int/lo}$Flt3$^+$M-CSFR$^-$ cells, c-Kit$^{int/lo}$Flt3$^+$M-CSFR$^+$ cells, and c-Kit$^+$Flt3$^+$M-CSFR$^+$ cells and were cultured in irradiated stromal cells Ac6 with Flt3-ligand and TPO for 8 days.

(C) Absolute numbers of pDC and cDC derived from different progenitors are shown. Error bars show the means ± SEM (n = 4 from two independent experiments). *p < 0.01.

See also Figure S6.

SUPPLEMENTAL INFORMATION

Supplemental Information includes Supplemental Experimental Procedures, six figures, and one table and can be found with this article online at http://dx.doi.org/10.1016/j.immuni.2013.04.006.

ACKNOWLEDGMENTS

We thank H. Kamioka for secretarial support and N. Sakaguchi (Kumamoto University) for the B6.*Rag1*$^{gfp/+}$ mice. This work was supported by the Sumitomo Foundation (N.O.), the Uehara Memorial Foundation (N.O.), the NOVARTIS foundation (N.O.), the Takeda Science Foundation (N.O., T.O.), a Grant-in-Aid for Scientific Research on Priority Areas from the Ministry of Education, Science, Sports and Culture of Japan (T.O.), and Japan Science and Technology Agency, Core Research for Evolutional Science and Technology (CREST) (T.O.).

Received: September 21, 2012
Accepted: April 3, 2013
Published: April 25, 2013

REFERENCES

Adolfsson, J., Månsson, R., Buza-Vidas, N., Hultquist, A., Liuba, K., Jensen, C.T., Bryder, D., Yang, L., Borge, O.J., Thoren, L.A., et al. (2005).

Identification of Flt3$^+$ lympho-myeloid stem cells lacking erythro-megakaryocytic potential a revised road map for adult blood lineage commitment. Cell *121*, 295–306.

Aliberti, J., Schulz, O., Pennington, D.J., Tsujimura, H., Reis e Sousa, C., Ozato, K., and Sher, A. (2003). Essential role for ICSBP in the in vivo development of murine CD8α^+ dendritic cells. Blood *101*, 305–310.

Anderson, K.L., Perkin, H., Surh, C.D., Venturini, S., Maki, R.A., and Torbett, B.E. (2000). Transcription factor PU.1 is necessary for development of thymic and myeloid progenitor-derived dendritic cells. J. Immunol. *164*, 1855–1861.

Asselin-Paturel, C., Boonstra, A., Dalod, M., Durand, I., Yessaad, N., Dezutter-Dambuyant, C., Vicari, A., O'Garra, A., Biron, C., Brière, F., and Trinchieri, G. (2001). Mouse type I IFN-producing cells are immature APCs with plasmacytoid morphology. Nat. Immunol. *2*, 1144–1150.

Auffray, C., Fogg, D.K., Narni-Mancinelli, E., Senechal, B., Trouillet, C., Saederup, N., Leemput, J., Bigot, K., Campisi, L., Abitbol, M., et al. (2009). CX_3CR1^+ CD115$^+$ CD135$^+$ common macrophage/DC precursors and the role of CX_3CR1 in their response to inflammation. J. Exp. Med. *206*, 595–606.

Banchereau, J., and Pascual, V. (2006). Type I interferon in systemic lupus erythematosus and other autoimmune diseases. Immunity *25*, 383–392.

Banchereau, J., and Steinman, R.M. (1998). Dendritic cells and the control of immunity. Nature *392*, 245–252.

Belz, G.T., and Nutt, S.L. (2012). Transcriptional programming of the dendritic cell network. Nat. Rev. Immunol. *12*, 101–113.

Björck, P. (2001). Isolation and characterization of plasmacytoid dendritic cells from Flt3 ligand and granulocyte-macrophage colony-stimulating factor-treated mice. Blood *98*, 3520–3526.

Bogunovic, M., Ginhoux, F., Helft, J., Shang, L., Hashimoto, D., Greter, M., Liu, K., Jakubzick, C., Ingersoll, M.A., Leboeuf, M., et al. (2009). Origin of the lamina propria dendritic cell network. Immunity *31*, 513–525.

Cella, M., Jarrossay, D., Facchetti, F., Alebardi, O., Nakajima, H., Lanzavecchia, A., and Colonna, M. (1999). Plasmacytoid monocytes migrate to inflamed lymph nodes and produce large amounts of type I interferon. Nat. Med. *5*, 919–923.

Chen, W., Antonenko, S., Sederstrom, J.M., Liang, X., Chan, A.S., Kanzler, H., Blom, B., Blazar, B.R., and Liu, Y.J. (2004). Thrombopoietin cooperates with FLT3-ligand in the generation of plasmacytoid dendritic cell precursors from human hematopoietic progenitors. Blood *103*, 2547–2553.

Cisse, B., Caton, M.L., Lehner, M., Maeda, T., Scheu, S., Locksley, R., Holmberg, D., Zweier, C., den Hollander, N.S., Kant, S.G., et al. (2008). Transcription factor E2-2 is an essential and specific regulator of plasmacytoid dendritic cell development. Cell *135*, 37–48.

D'Amico, A., and Wu, L. (2003). The early progenitors of mouse dendritic cells and plasmacytoid predendritic cells are within the bone marrow hemopoietic precursors expressing Flt3. J. Exp. Med. *198*, 293–303.

de Heer, H.J., Hammad, H., Soullié, T., Hijdra, D., Vos, N., Willart, M.A., Hoogsteden, H.C., and Lambrecht, B.N. (2004). Essential role of lung plasmacytoid dendritic cells in preventing asthmatic reactions to harmless inhaled antigen. J. Exp. Med. *200*, 89–98.

Edelson, B.T., KC, W., Juang, R., Kohyama, M., Benoit, L.A., Klekotka, P.A., Moon, C., Albring, J.C., Ise, W., Michael, D.G., et al. (2010). Peripheral CD103+ dendritic cells form a unified subset developmentally related to CD8α+ conventional dendritic cells. J. Exp. Med. *207*, 823–836.

Fancke, B., Suter, M., Hochrein, H., and O'Keeffe, M. (2008). M-CSF: a novel plasmacytoid and conventional dendritic cell poietin. Blood *111*, 150–159.

Fogg, D.K., Sibon, C., Miled, C., Jung, S., Aucouturier, P., Littman, D.R., Cumano, A., and Geissmann, F. (2006). A clonogenic bone marrow progenitor specific for macrophages and dendritic cells. Science *311*, 83–87.

Geissmann, F., Manz, M.G., Jung, S., Sieweke, M.H., Merad, M., and Ley, K. (2010). Development of monocytes, macrophages, and dendritic cells. Science *327*, 656–661.

Ghosh, H.S., Cisse, B., Bunin, A., Lewis, K.L., and Reizis, B. (2010). Continuous expression of the transcription factor E2-2 maintains the cell fate of mature plasmacytoid dendritic cells. Immunity *33*, 905–916.

Gilliet, M., Cao, W., and Liu, Y.J. (2008). Plasmacytoid dendritic cells: sensing nucleic acids in viral infection and autoimmune diseases. Nat. Rev. Immunol. *8*, 594–606.

Ginhoux, F., Liu, K., Helft, J., Bogunovic, M., Greter, M., Hashimoto, D., Price, J., Yin, N., Bromberg, J., Lira, S.A., et al. (2009). The origin and development of nonlymphoid tissue CD103+ DCs. J. Exp. Med. *206*, 3115–3130.

Goubier, A., Dubois, B., Gheit, H., Joubert, G., Villard-Truc, F., Asselin-Paturel, C., Trinchieri, G., and Kaiserlian, D. (2008). Plasmacytoid dendritic cells mediate oral tolerance. Immunity *29*, 464–475.

Guerriero, A., Langmuir, P.B., Spain, L.M., and Scott, E.W. (2000). PU.1 is required for myeloid-derived but not lymphoid-derived dendritic cells. Blood *95*, 879–885.

Hildner, K., Edelson, B.T., Purtha, W.E., Diamond, M., Matsushita, H., Kohyama, M., Calderon, B., Schraml, B.U., Unanue, E.R., Diamond, M.S., et al. (2008). Batf3 deficiency reveals a critical role for CD8α+ dendritic cells in cytotoxic T cell immunity. Science *322*, 1097–1100.

Jung, S., Aliberti, J., Graemmel, P., Sunshine, M.J., Kreutzberg, G.W., Sher, A., and Littman, D.R. (2000). Analysis of fractalkine receptor CX(3)CR1 function by targeted deletion and green fluorescent protein reporter gene insertion. Mol. Cell. Biol. *20*, 4106–4114.

Karsunky, H., Merad, M., Cozzio, A., Weissman, I.L., and Manz, M.G. (2003). Flt3 ligand regulates dendritic cell development from Flt3+ lymphoid and myeloid-committed progenitors to Flt3+ dendritic cells in vivo. J. Exp. Med. *198*, 305–313.

Kushida, T., Inaba, M., Hisha, H., Ichioka, N., Esumi, T., Ogawa, R., Iida, H., and Ikehara, S. (2001). Intra-bone marrow injection of allogeneic bone marrow cells: a powerful new strategy for treatment of intractable autoimmune diseases in MRL/lpr mice. Blood *97*, 3292–3299.

Kuwata, N., Igarashi, H., Ohmura, T., Aizawa, S., and Sakaguchi, N. (1999). Cutting edge: absence of expression of RAG1 in peritoneal B-1 cells detected by knocking into RAG1 locus with green fluorescent protein gene. J. Immunol. *163*, 6355–6359.

Liu, Y.J. (2005). IPC: professional type 1 interferon-producing cells and plasmacytoid dendritic cell precursors. Annu. Rev. Immunol. *23*, 275–306.

Liu, K., Victora, G.D., Schwickert, T.A., Guermonprez, P., Meredith, M.M., Yao, K., Chu, F.F., Randolph, G.J., Rudensky, A.Y., and Nussenzweig, M. (2009). In vivo analysis of dendritic cell development and homeostasis. Science *324*, 392–397.

McKenna, H.J., Stocking, K.L., Miller, R.E., Brasel, K., De Smedt, T., Maraskovsky, E., Maliszewski, C.R., Lynch, D.H., Smith, J., Pulendran, B., et al. (2000). Mice lacking flt3 ligand have deficient hematopoiesis affecting hematopoietic progenitor cells, dendritic cells, and natural killer cells. Blood *95*, 3489–3497.

Merad, M., and Manz, M.G. (2009). Dendritic cell homeostasis. Blood *113*, 3418–3427.

Nagasawa, M., Schmidlin, H., Hazekamp, M.G., Schotte, R., and Blom, B. (2008). Development of human plasmacytoid dendritic cells depends on the combined action of the basic helix-loop-helix factor E2-2 and the Ets factor Spi-B. Eur. J. Immunol. *38*, 2389–2400.

Naik, S.H., Metcalf, D., van Nieuwenhuijze, A., Wicks, I., Wu, L., O'Keeffe, M., and Shortman, K. (2006). Intrasplenic steady-state dendritic cell precursors that are distinct from monocytes. Nat. Immunol. *7*, 663–671.

Naik, S.H., Sathe, P., Park, H.Y., Metcalf, D., Proietto, A.I., Dakic, A., Carotta, S., O'Keeffe, M., Bahlo, M., Papenfuss, A., et al. (2007). Development of plasmacytoid and conventional dendritic cell subtypes from single precursor cells derived in vitro and in vivo. Nat. Immunol. *8*, 1217–1226.

Nakano, H., Yanagita, M., and Gunn, M.D. (2001). CD11c(+)B220(+)Gr-1(+) cells in mouse lymph nodes and spleen display characteristics of plasmacytoid dendritic cells. J. Exp. Med. *194*, 1171–1178.

Onai, N., Obata-Onai, A., Tussiwand, R., Lanzavecchia, A., and Manz, M.G. (2006). Activation of the Flt3 signal transduction cascade rescues and enhances type I interferon-producing and dendritic cell development. J. Exp. Med. *203*, 227–238.

Onai, N., Obata-Onai, A., Schmid, M.A., Ohteki, T., Jarrossay, D., and Manz, M.G. (2007). Identification of clonogenic common Flt3+M-CSFR+ plasmacytoid and conventional dendritic cell progenitors in mouse bone marrow. Nat. Immunol. *8*, 1207–1216.

Ovchinnikov, D.A., DeBats, C.E., Sester, D.P., Sweet, M.J., and Hume, D.A. (2010). A conserved distal segment of the mouse CSF-1 receptor promoter is required for maximal expression of a reporter gene in macrophages and osteoclasts of transgenic mice. J. Leukoc. Biol. *87*, 815–822.

Pelayo, R., Hirose, J., Huang, J., Garrett, K.P., Delogu, A., Busslinger, M., and Kincade, P.W. (2005). Derivation of 2 categories of plasmacytoid dendritic cells in murine bone marrow. Blood *105*, 4407–4415.

Reizis, B. (2010). Regulation of plasmacytoid dendritic cell development. Curr. Opin. Immunol. *22*, 206–211.

Schiavoni, G., Mattei, F., Sestili, P., Borghi, P., Venditti, M., Morse, H.C., 3rd, Belardelli, F., and Gabriele, L. (2002). ICSBP is essential for the development of mouse type I interferon-producing cells and for the generation and activation of CD8α(+) dendritic cells. J. Exp. Med. *196*, 1415–1425.

Schiavoni, G., Mattei, F., Borghi, P., Sestili, P., Venditti, M., Morse, H.C., 3rd, Belardelli, F., and Gabriele, L. (2004). ICSBP is critically involved in the normal development and trafficking of Langerhans cells and dermal dendritic cells. Blood *103*, 2221–2228.

Schlitzer, A., Loschko, J., Mair, K., Vogelmann, R., Henkel, L., Einwächter, H., Schiemann, M., Niess, J.H., Reindl, W., and Krug, A. (2011). Identification of CCR9- murine plasmacytoid DC precursors with plasticity to differentiate into conventional DCs. Blood *117*, 6562–6570.

Schlitzer, A., Heiseke, A.F., Einwächter, H., Reindl, W., Schiemann, M., Manta, C.-P., See, P., Niess, J.H., Suter, T., Ginhoux, F., and Krug, A.B. (2012). Tissue-specific differentiation of a circulating CCR9- pDC-like common dendritic cell precursor. Blood *119*, 6063–6071.

Shortman, K., and Naik, S.H. (2007). Steady-state and inflammatory dendritic-cell development. Nat. Rev. Immunol. *7*, 19–30.

Siegal, F.P., Kadowaki, N., Shodell, M., Fitzgerald-Bocarsly, P.A., Shah, K., Ho, S., Antonenko, S., and Liu, Y.J. (1999). The nature of the principal type 1 interferon-producing cells in human blood. Science *284*, 1835–1837.

Swiecki, M., and Colonna, M. (2010). Unraveling the functions of plasmacytoid dendritic cells during viral infections, autoimmunity, and tolerance. Immunol. Rev. *234*, 142–162.

Toyama-Sorimachi, N., Tsujimura, Y., Maruya, M., Onoda, A., Kubota, T., Koyasu, S., Inaba, K., and Karasuyama, H. (2004). Ly49Q, a member of the Ly49 family that is selectively expressed on myeloid lineage cells and involved in regulation of cytoskeletal architecture. Proc. Natl. Acad. Sci. USA *101*, 1016–1021.

Tsujimura, H., Tamura, T., and Ozato, K. (2003). Cutting edge: IFN consensus sequence binding protein/IFN regulatory factor 8 drives the development of type I IFN-producing plasmacytoid dendritic cells. J. Immunol. *170*, 1131–1135.

Varol, C., Vallon-Eberhard, A., Elinav, E., Aychek, T., Shapira, Y., Luche, H., Fehling, H.J., Hardt, W.D., Shakhar, G., and Jung, S. (2009). Intestinal lamina propria dendritic cell subsets have different origin and functions. Immunity *31*, 502–512.

Waskow, C., Liu, K., Darrasse-Jèze, G., Guermonprez, P., Ginhoux, F., Merad, M., Shengelia, T., Yao, K., and Nussenzweig, M. (2008). The receptor tyrosine kinase Flt3 is required for dendritic cell development in peripheral lymphoid tissues. Nat. Immunol. *9*, 676–683.

Watowich, S.S., and Liu, Y.J. (2010). Mechanisms regulating dendritic cell specification and development. Immunol. Rev. *238*, 76–92.

Wilson, A., Laurenti, E., Oser, G., van der Wath, R.C., Blanco-Bose, W., Jaworski, M., Offner, S., Dunant, C.F., Eshkind, L., Bockamp, E., et al. (2008). Hematopoietic stem cells reversibly switch from dormancy to self-renewal during homeostasis and repair. Cell *135*, 1118–1129.

Zhang, J., Raper, A., Sugita, N., Hingorani, R., Salio, M., Palmowski, M.J., Cerundolo, V., and Crocker, P.R. (2006). Characterization of Siglec-H as a novel endocytic receptor expressed on murine plasmacytoid dendritic cell precursors. Blood *107*, 3600–3608.